EUROPEAN JOURNAL OF PURE AND APPLIED MATHEMATICS
Vol. 16, No. 4, 2023, 2775-2785
ISSN 1307-5543 – ejpam.com
Published by New York Business Global

Study on the dynamical analysis of a family of third-order multiple zero finders

Young Hee Geum

Department of Mathematics, Dankook University, Cheonan, Korea 330-714

Abstract. We study the complex dynamics by analyzing the dynamical planes associated with the family of third order multiple root finders and the parameter spaces related to the free critical points. The conjugacy maps with the theoretical results of dynamical analysis for the iterative schemes are investigated. In addition, the various experiments are implemented to draw the dynamics of the cubic-order schemes as well as existing methods.

2020 Mathematics Subject Classifications: 65H05, 65H99

Key Words and Phrases: Conjugacy map, basins of attraction, multiple root, nonlinear equation, parameter space, Blood Rheology model

---

1. Introduction

Many real-world problems involve finding solutions [1, 4, 17, 19] to equations. These equations can represent physical, biological, economic, and other systems. The root-finding problem[3, 10, 14] is a fundamental and crucial concept in mathematics, engineering, computer science, and various scientific disciplines. Root-finding algorithms[3] help us find the points where these equations cross zero, which often correspond to critical points or solutions of the underlying problem. The modified Newton scheme is the effective method to compute multiple roots given by

$$x_{n+1} = x_n - m\frac{f(x)}{f'(x)}.$$

The scholars [2, 5, 7, 16, 20] are studying the dynamical problems of finding multiple zeros of nonlinear equations. The dynamical behavior of nonlinear equations[15] are found in many fields, such as artificial intelligence, engineering, medicine, and satellites.

The following third-order method[11] given by

$$\begin{cases} x_{n+1} = x_n - \frac{mf(y_n)}{t^m f'(x_n)}, \\ y_n = x_n - m(1-t)\frac{f(x_n)}{f'(x_n)}, \end{cases} \tag{1}$$

DOI: https://doi.org/10.29020/nybg.ejpam.v16i4.4986

Email address: `conpana@empal.com` (Y.H. Geum)

is pursued its dynamics by constructing the conjugacy map.

Osada's third-order method[16] is written as

$$x_{n+1} = x_n - \frac{1}{2}m(m+1)\frac{f(x_n)}{f'(x_n)} + \frac{1}{2}(m-1)^2\frac{f'(x_n)}{f''(x_n)}. \tag{2}$$

Dong's third-order method [7] is given by

$$\begin{cases} x_{n+1} = z_n - (1 - \frac{1}{\sqrt{m}})^{1-m}\frac{f(z_n)}{f'(z_n)}, \\ z_n = x_n - \sqrt{m}\frac{f(x_n)}{f'(x_n)}. \end{cases} \tag{3}$$

Let $g : X \to X$ and $h : Y \to Y$ be two analytic functions. The functions g and h are said to be topologically conjugate if there exists a homeomorphism $k : X \to Y$ such that $k \circ g = h \circ k$, where $\circ$ denotes function composition. Then the map k is called a conjugacy [4]. Then, $h = k \circ g \circ k^{-1}$ and $h^n = k \circ g^n \circ k^{-1}$. If g is topologically conjugate to h via k and ν is a fixed point of h, then $k^{-1}(\nu)$ is a fixed point of g. If g and h are invertible, then the topological conjugacy k maps an orbit of g onto an orbit of h and the order of points is preserved.

In this paper, we study the dynamics of the parameter space of the following cubic order iterative method developed in [9] for finding multiple roots using the conjugacy map.

$$\begin{cases} y_n = x_n - m(1-t)\frac{f(x_n)}{f'(x_n)}, \\ x_{n+1} = x_n - \frac{f(y_n)+(m-t^m)f(x_n)}{f'(x_n)}. \end{cases} \tag{4}$$

The rest of this work is organized as follows. In section 2, we construct the conjugacy map and the stability surfaces are shown. Section 3 describes the complex dynamical analysis including the parameter spaces and the basins of attraction. In the last section, we describe the future work by investigating the dynamical analysis from the diverse viewpoints.

2. Dynamical Analysis

A nonlinear equation (4) is reformed as a discrete dynamical system:

$$x_{n+1} = I_f(x_n), \tag{5}$$

where I_f is the iterative method. We have a complex discrete dynamical system

$$z_{n+1} = I_f(z_n) = z_n - \frac{f(y_n) + \gamma f(z_n)}{f'(z_n)}, \tag{6}$$

where $y_n = z_n - \mu h(z_n), \mu = m(1-t), h(z_n) = \frac{f(z_n)}{f'(z_n)}$ and $\gamma = m - t^m$.

For $M(z) = \frac{z-A}{z-B}$ and $f(z) = (z-A)^m(z-B)^m$ with $m \in N$ [6], we have

$$J(z,t) = M \circ I_f \circ M^{-1}(z) = \frac{z(r_1r_2 - r_3\mu_1)}{zr_1r_2 - r_3\mu_2}, \tag{7}$$

where $r_1 = (t+z)^m$, $r_2 = (1+tz)^m$, $r_3 = (1+z)^{2m}$, $\mu_1 = t^m + mz$ and $\mu_2 = m + t^m z$ and $A,\ B \in \mathbb{C} \cup \{\infty\}, A \neq B$. Then $I_f(z,t)$ is conjugate to $J(z,t)$.

Using the inverse of $M(z)$, that is $M^{-1}(z) = \frac{Bz-A}{z-1}$, we have the following form:

$$J(z,t) = \begin{cases} \frac{(-2+t-z)z^2(t+z)}{(-1+(-2+t)z)(1+tz)}, & \text{m=1}, \\ \frac{z(t^2(1+z)^4+2z(1+z)^4-(t+z)^2(1+tz)^2)}{2(1+z)^4+t^2z(1+z)^4-z(t+z)^2(1+tz)^2}, & \text{m=2}. \end{cases} \tag{8}$$

We find out that $z = 0$ and $z = \infty$ are the fixed points of the conjugate map $J(z,t)$, regardless of t-values. By a lengthy and accurate computation [18], we have that $z = 1$ is a strange fixed point of J which is not a zero of $f(z) = (z-A)^m(z-B)^m$, regardless of t-values.

We will find the fixed points of the iterative scheme $J(z,t)$. Let $\phi(z,t) = J(z,t) - z$, whose roots are the fixed points of J.

$$\phi(z,t) = -\frac{z(z-1)(r_1r_2 - r_3\mu_3)}{zr_1r_2 - r_3\mu_3}, \tag{9}$$

with $\mu_3 = t^m - m$. We find that $z = 0$ and $z = 1$ are the roots of ϕ.

To study the dynamical analysis behind iterative map (1) applied to a quadratic polynomial raised to the power of m, $f(z) = (z-A)^m(z-B)^m$, we will consider the fixed points of J and their stability. For $m \in \{1,2\}$, we have the explicit form of $\phi(z,t)$ satisfying

$$\phi(z,t) = \begin{cases} \frac{z(z-1)\psi_1(z)}{q_1(z)}, & \text{if} \quad \text{m=1}, \\ \frac{z(z-1)\psi_2(z)}{q_2(z)}, & \text{if} \quad \text{m=2}, \end{cases} \tag{10}$$

where

$$\begin{aligned}
&\psi_1(z) = -(1 + (3-2t+t^2)z + z^2), \\
&q_1(z) = -1 - 2z + (-2t+t^2)z^2, \\
&\psi_2(z) = 2 + (8+2t-4t^2+2t^3)z + (13-2t^2+t^4)z^2 + (8+2t-4t^2+2t^3)z^3 + z^4, \\
&q_2(z) = 2 + 8z + (12-2t+4t^2-2t^3)z^2 + (7+2t^2-t^4)z^3 + (2-2t+4t^2-2t^3)z^4.
\end{aligned}$$

Suppose $\psi_1(z) = 0$ and $q_1(z) = 0$, for some value of z. By eliminating t from two polynomials, we get $W(z) = (z+1)^3$. Substituting the roots of $W(z)$ into $\psi_1(z) = 0$ and $q_1(z) = 0$, we get the relations for t. Solving them for t, we have $t = 1$. For $t \neq 1$, $\psi_1(\frac{1}{z}) = z^{-2}\psi_1(z)$. If $z \neq 0$ is a root of $\psi_1(z)$, then so is $\frac{1}{z}$. In case of $m = 2$, we have $W(z) = (z+1)^5$ and $\psi_2(\frac{1}{z}) = z^{-4}\psi_2(z)$ through a similar process.

We have that $J'(z,t)$ can be reformed a fraction as follows:

$$J'(z,t) = \frac{mr_3(mz(-(-1+t)^2(-1+z)^2 r_1^{\frac{-1+m}{m}} r_2^{\frac{-1+m}{m}} + 2r_3) + (1+z^2)(-r_1r_2 + t^m r_3))}{(zr_1r_2 - (m+t^m z)r_3)^2}. \tag{11}$$

We will draw the stability surfaces of the fixed points. The stability surfaces of the fixed points are shown by conical surfaces in Figures 1 - 2.

Computing the derivative of J, we obtain the following relations

$$J'(z,t) = \begin{cases} \frac{2z(z+1)^2 Q_1(z)}{w_1(z)^2}, & \text{if} \quad \text{m=1}, \\ \frac{2z(z+1)^4 Q_2(z)}{w_2(z)^2}, & \text{if} \quad \text{m=2}, \end{cases} \tag{12}$$

where

$$\begin{aligned} Q_1(z) &= -((-2+t)t) + (3-2t+t^2)z - (-2+t)tz^2, \\ Q_2(z) &= -4(-1+t-2t^2+t^3) + (13+8t-10t^2+8t^3-3t^4)z \\ &\quad + 4(7-4t+6t^2-4t^3+t^4)z^2 + (13+8t-10t^2+8t^3 \\ &\quad - 3t^4)z^3 - 4(-1+t-2t^2+t^3)z^4, \\ w_1(z) &= 1 + (4-t)z - (-2+t)(2+t)z^2 + (-2+t)^2 tz^3, \\ w_2(z) &= -2 - 8z + 2(-6+t-2t^2+t^3)z^2 + (-7-2t^2+t^4)z^3 + 2(-1+t-2t^2+t^3)z^4. \end{aligned}$$

The critical points of the numerical method refers to a point where the derivative of a function is zero, that is $J'(z,t) = 0$. The points $z = 0$ and $z = \infty$ are critical points associated with $(z-A)(z-B)$. The critical points that are not any roots of the polynomial $(z-A)(z-B)$ are said to be free critical points.

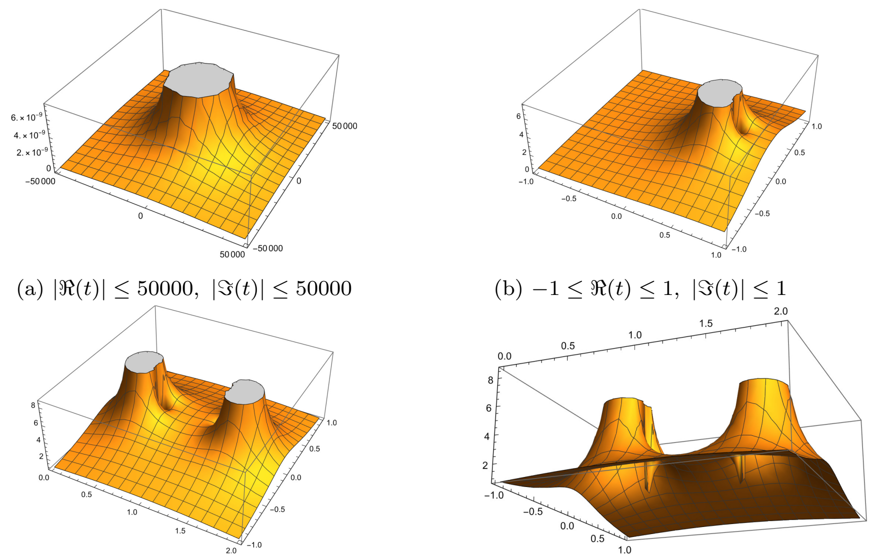

(a) $|\Re(t)| \le 50000, \ |\Im(t)| \le 50000$
(b) $-1 \le \Re(t) \le 1, \ |\Im(t)| \le 1$
(c) $0 \le |\Re(t)| \le 2, \ -1 \le |\Im(t)| \le 1$
(d) $0 \le |\Re(t)| \le 2, \ -1 \le |\Im(t)| \le 1$

Figure 1: Stability surfaces for $m = 1$.

We describe the complex dynamical behavior from the viewpoint of parameter spaces and dynamical plane. The following theorems will be useful to confirm the properties of symmetry on dynamical planes and parameter spaces.

Let $\mathcal{D} = \{z \in C : \textit{an orbit of } z \textit{ under } J(z,t) \textit{ tends to a number } \eta_d \textit{ in } \overline{C}\}$ as the dynamical plane and let $\mathcal{P} = \{t \in C : \textit{a critical orbit of } z \textit{ under } J(z,t) \textit{ tends to a number } \eta_p \textit{ in } \overline{C}\}$ as the parameter space [12, 13]. If the number η_d or η_p is a finite constant, there exist finite periods in the orbit. Otherwise, the orbits go to infinity or are periodic but bounded. We consider $z = \infty$ as a fixed point in Riemann sphere.

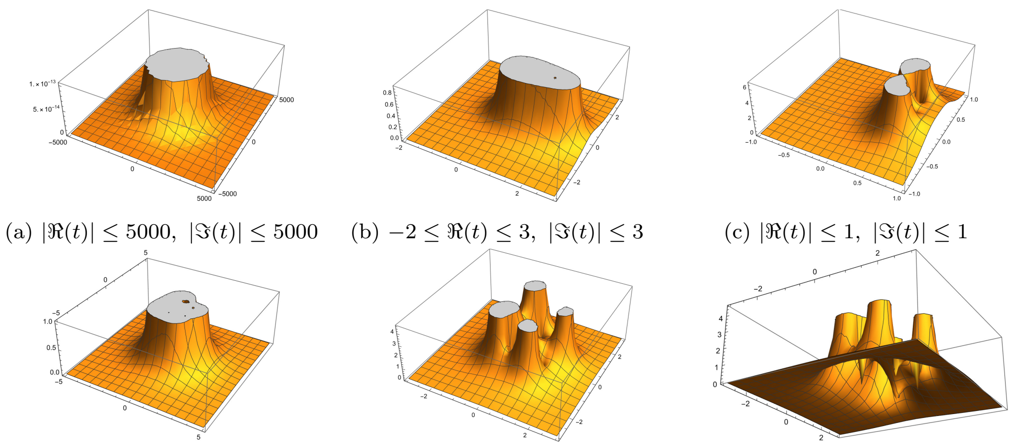

(a) $|\Re(t)| \leq 5000,\ |\Im(t)| \leq 5000$ (b) $-2 \leq \Re(t) \leq 3,\ |\Im(t)| \leq 3$ (c) $|\Re(t)| \leq 1,\ |\Im(t)| \leq 1$

(d) $|\Re(t)| \leq 5,\ |\Im(t)| \leq 5$ (e) $|\Re(t)| \leq 3,\ |\Im(t)| \leq 3$ (f) $|\Re(t)| \leq 3,\ |\Im(t)| \leq 3$

Figure 2: Stability surfaces for $m = 2$.

Theorem 1. *Let $z(t)$ be a point of iterative map $J(z,t)$ where $t \in R$. Then the dynamical plane is symmetric with respect to its horizontal axis.*

Proof. Considering $\bar{t} = t$, We have $J(z,t)$:

$$|J(z,t)| = |\overline{J(z,t)}| = |J(\overline{z},\overline{t}| = |J(\overline{z},t)|,$$

which means that the magnitude of the orbit of $z(t)$ is the same as that of the orbit of $\overline{z(t)}$. Then the dynamical plane related to map $J(z,t)$ is symmetric with respect to its horizontal axis if t is real.

Theorem 2. *Let $z(t)$ be a free critical point of $J(z,t)$ depending on parameter t by a root of $Q(z) = 0$. Then the parameter space is symmetric with respect to its horizontal axis.*

Proof. For $m = 2$, we have $z(t)$ is a zero of $Q_2(z)$ for a given t. Then $\overline{z}(\overline{t})$ is a root of $Q(z)$ at $\overline{t}$. For a free critical point $z(t)$, we have the conjugated map $J(z,t)$ from (8). Then

$$|J(z,t)| = |J(z(t),t)| = |\overline{J(z(t),t)}| = |J(\overline{z(t)},\overline{t}| = |J(\overline{z}((\overline{t}),\overline{t})|,$$

which implies that the magnitude of the orbit of free critical point z is the same as that of the orbit of free critical point $\overline{z}$ at $\overline{t}$. It states that the corresponding parameter space is symmetric with respect to its horizontal axis.

We develop a systematic color palette in Table 1 to paint a point $t \in \mathcal{P}$ according to the orbital period of z of $J(z,t)$ for $t \in \mathcal{P}$. Then the point t is determined by the corresponding color C_k if t induces a k-periodic orbit with $k \in \mathbb{N} \cup \{0\}$ under $J(z,t)$. We use a tolerance of 10^{-6} after up to 1000 iterations to allow for desired k periodic convergence of an orbit[1, 18] associated with $\mathcal{P}$. In this experiments, we draw the color C_q using the color palette in Table 1

Table 1: Color palette for a q-periodic orbit with $q \in \mathbb{N} \cup \{0\}$

q	C_q
$q = 1$	$C_1 = \begin{cases} \text{magenta, for fixed point } \infty \\ \text{cyan, for fixed point } 0 \\ \text{yellow, for fixed point } 1 \\ \text{red, for other strange fixed point ,} \end{cases}$
$2 \le q \le 68$	C_2 = orange, C_3 = light green, C_4 = dark red, C_5 = dark blue, C_6 = dark green, C_7 = dark yellow, C_8 = floral white, C_9 = light pink, C_{10} = khaki, C_{11} = dark orange, C_{12} = turquoise, C_{13} = lavender, C_{14} = thistle, C_{15} = plum, C_{16} = orchid, C_{17} = medium orchid, C_{18} = blue violet, C_{19} = dark orchid, C_{20} = purple, C_{21} = power blue, C_{22} = sky blue, C_{23} = deep sky blue, C_{24} = dodger blue, C_{25} = royal blue, C_{26} = medium spring green, C_{27} = spring green, C_{28} = medium sea green, C_{29} = sea green, C_{30} = forest green, C_{31} = olive drab, C_{32} = bisque, C_{33} = moccasin, C_{34} = light salmon, C_{35} = salmon, C_{36} = light coral, C_{37} = Indian red, C_{38} = brown, C_{39} = fire brick, C_{40} = peach puff, C_{41} = wheat, C_{42} = sandy brown, C_{43} = tomato, C_{44} = orange red, C_{45} = chocolate, C_{46} = pink, C_{47} = pale violet red, C_{48} = deep pink, C_{49} = violet red, C_{50} = gainsboro, C_{51} = light gray, C_{52} = dark gray, C_{53} = gray, C_{54} = charteruse, C_{55} = electric indigo, C_{56} = electric lime, C_{57} = lime, C_{58} = silver, C_{59} = teal, C_{60} = pale turquoise, C_{61} = sandy brown, C_{62} = honeydew, C_{63} = misty rose, C_{64} = lemon chiffon, C_{65} = lavender blush, C_{66} = gold, C_{67} = crimson, C_{68} = tan.
$q = 0^*$ or $q > 69$	C_q = black.

$*$: $q = 0$: the orbit is non-periodic but bounded.

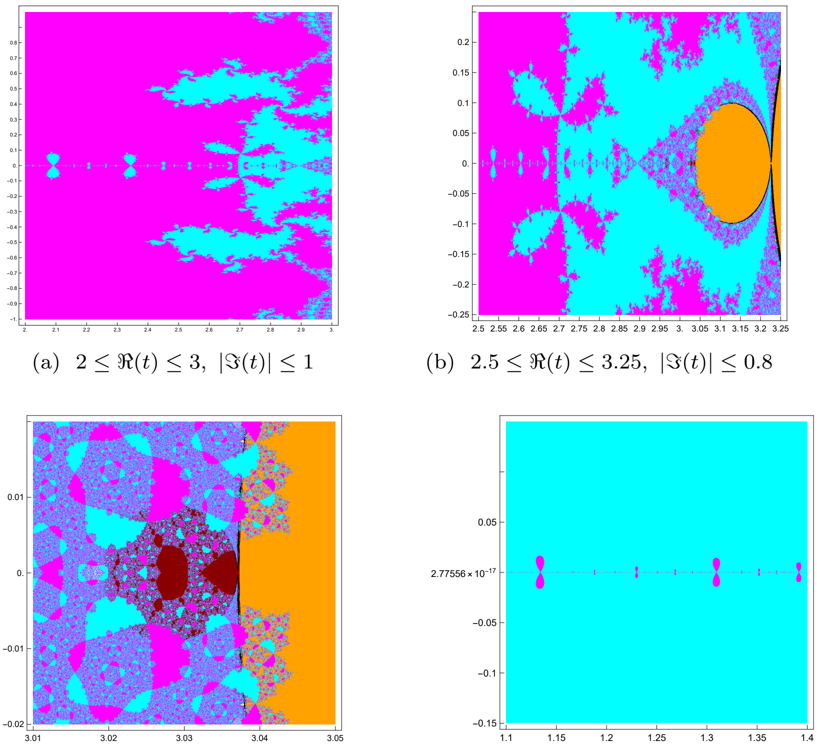

(a) $2 \le \Re(t) \le 3,\ |\Im(t)| \le 1$

(b) $2.5 \le \Re(t) \le 3.25,\ |\Im(t)| \le 0.8$

(c) $3.01 \le \Re(t) \le 3.05,\ |\Im(t)| \le 0.2$

(d) $1.1 \le \Re(t) \le 1.4,\ |\Im(t)| \le 0.15$

Figure 3: Parameter space for $m = 1$.

In Figures 3–4, the related parameter spaces $\mathcal{P}$ for $m = 1, 2$ are displayed. A point $t \in \mathcal{P}$ is determined by the color palette in Table 1. In terms of numerical experiments, every point of the parameter space $\mathcal{P}$ whose color is none of cyan(root $z = A$), magenta(root $z = B$), yellow or red is not a better choice of t. Let $\mathcal{P}_i$ denote the parameter space associated with branch cp_i for $1 \le i \le 4$. We figure out that $n \in \{2, 3, \cdots\}$ periodic orbit is budding at the main component(period-1 component) and 4-periodic component is budding at period-2 component.

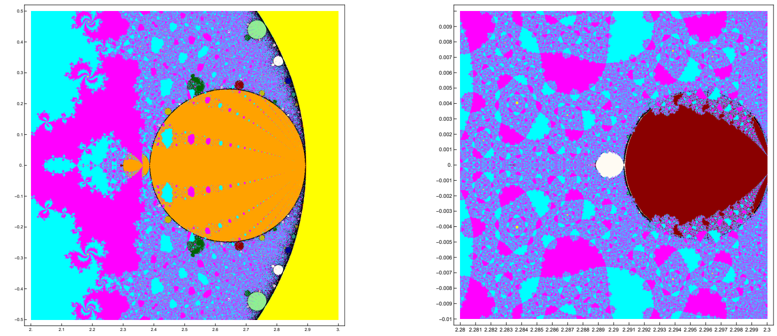

(a) $2 \le \Re(t)| \le 3,\ |\Im(t)| \le 0.5$ (b) $2.28 \le \Re(t) \le 2.3,\ |\Im(t)| \le 0.01$

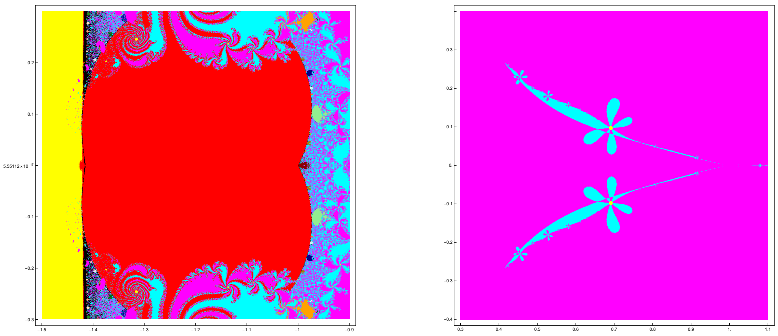

(c) $-1.5 \le \Re(t) \le 0.9,\ |\Im(t)| \le 0.3$ (d) $0.3 \le \Re(t) \le 1.1,\ |\Im(t)| \le 0.4$

Figure 4: Parameter space for $m = 2$.

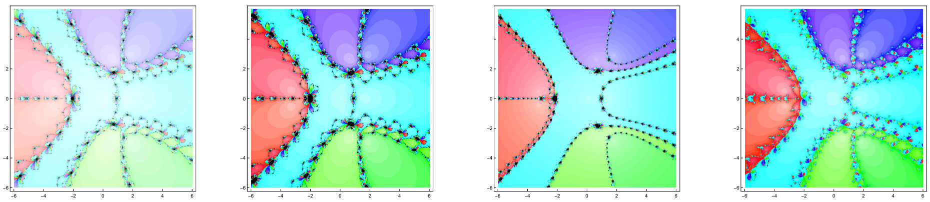

(a) $y1$ (b) $y2$ (c) $d1$ (d) $o1$

Figure 5: Basins of attraction of Blood Rheology model

We compare the proposed scheme(y1) in (4) with the third order method(y2) in (1), the Dong's third-order method(d1) in (2) and the Osada's scheme(o1) in (3) based on the dynamical analysis. We have taken the test functions having multiple roots with multiplicity $m = 2, 3, 4, 5, 6$ to draw the complex dynamics of the proposed method[9] y1,

Table 2: Test functions

p_δ	**method**	**time**	**con**	**no**	**div**
p_1	y1	78.937	359,555	7.63739	445
	y2	75.516	359,554	7.4628	446
	d1	150.359	352,420	10.7719	7,580
	o1	74.046	339,770	12.244	20,230
p_2	y1	126.313	359,998	5.97738	2
	y2	43.64	359,910	6.00031	90
	d1	117.625	359,963	11.2723	37
	o1	48.094	360,000	6.20214	0
p_3	y1	101.485	359,894	6.36682	106
	y2	115.391	359,757	8.37467	243
	d1	165.921	355,194	11.243	4,806
	o1	52.954	356,058	10.3829	3,942
p_4	y1	83.797	360,000	6.05845	0
	y2	54.844	358.860	5.9645	1,140
	d1	544.218	5,263	20.4971	354,737
	o1	46.219	360,000	6.17781	0
p_5	y1	104.625	359,937	6.84216	63
	y2	62.781	358,867	5.97515	1133
	d1	607.906	1,057	8.1211	358,943
	o1	676.015	188	12.6383	359,812

$p_1(z) = (z^7 - 9)^2$, $p_2(z) = (z^2 - 3z + 5)^3$, $p_3(z) = (z^5 - 6)^4$,
$p_4(z) = (z^2 + 3z + 7)^5$, $p_5(z) = (z^2 + 3z + 5)^6$.

Table 3: Blood Rheology model

b_δ	**method**	**time**	**con**	**no**	**div**
b_1	y1	486.844	359,920	9.54763	80
	y2	631.36	351,124	8.70651	8,876
	d1	1014.52	355,602	17.8899	4,398
	o1	233.89	359,910	9.85888	90

y2, Dong's scheme and Osada's method with the basins of attraction. In this statistical Table 2 for the basins of attraction, abbreviations **time**, **con**, **no** and **div** denote the value of CPU time for convergence, the value of total convergent points, the value of average iteration number for convergence and the value of divergent points.

As the first example, we select the polynomial $p_1(z) = (z^7 - 9)^2$ with roots $z = -1.23319 \pm 0.593873i, -0.304573 \pm 1.33442i, 0.853394 \pm 1.07012i, 1.36874$ of multiplicity $m = 2$. The method y1 is better in view of con. As the next instance, the polynomial $p_2(z) = (z^2 - 3z + 5)^3$ has the roots $z = 1/2(3 \pm i\sqrt{11})$. The method y1 is better in view of no. We select $p_3(z) = (z^5 - 6)^4$ with the roots $z = -1.15768 \pm 0.841103i, 0.442194 \pm 1.36093i, 1.43097$ and $p_4(z) = (z^2 + 3z + 7)^5, z = \frac{1}{2}(-3 \pm i\sqrt{19})$. As the last test function,

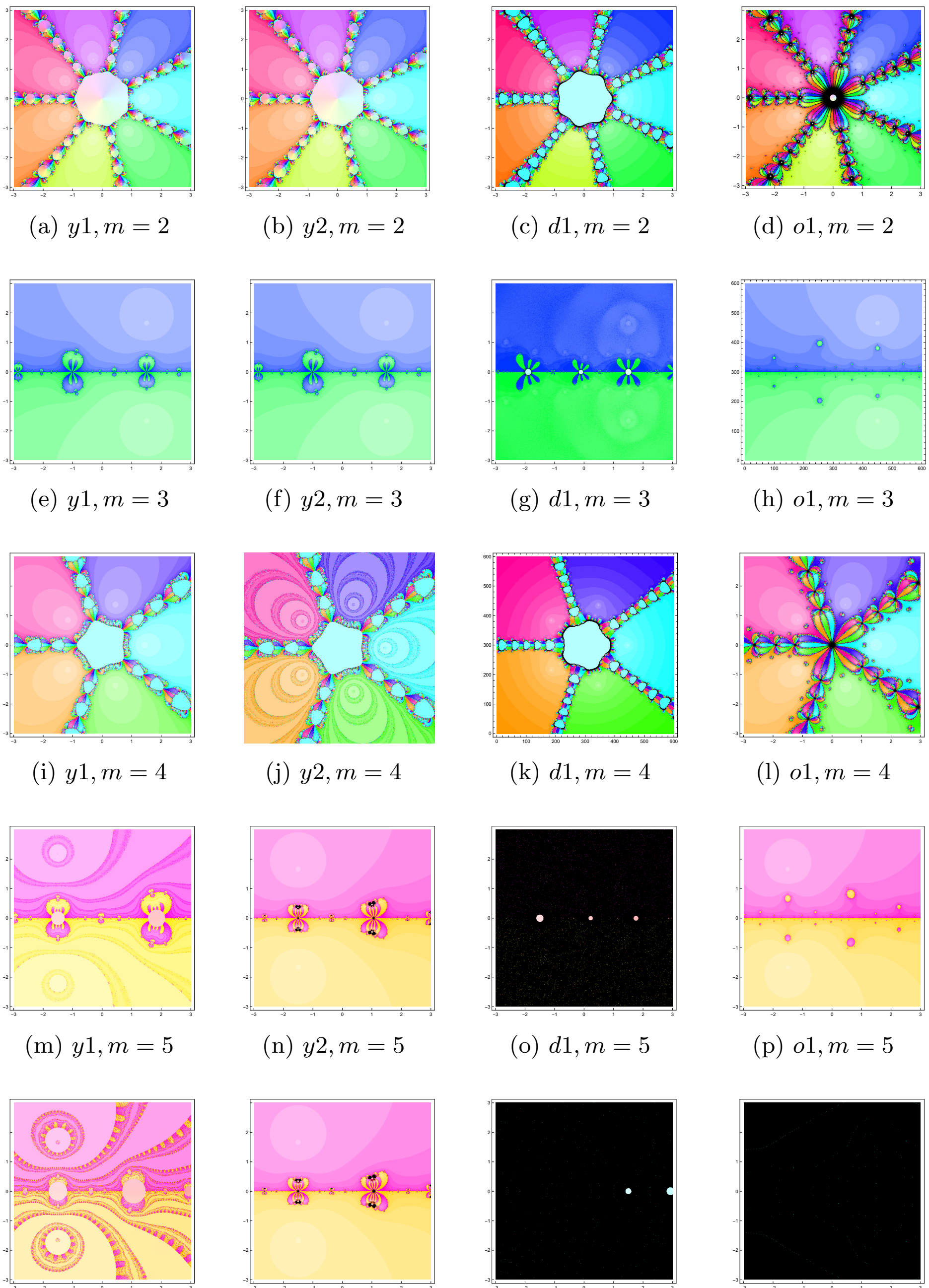

(a) $y1, m = 2$ (b) $y2, m = 2$ (c) $d1, m = 2$ (d) $o1, m = 2$

(e) $y1, m = 3$ (f) $y2, m = 3$ (g) $d1, m = 3$ (h) $o1, m = 3$

(i) $y1, m = 4$ (j) $y2, m = 4$ (k) $d1, m = 4$ (l) $o1, m = 4$

(m) $y1, m = 5$ (n) $y2, m = 5$ (o) $d1, m = 5$ (p) $o1, m = 5$

(q) $y1, m = 6$ (r) $y2, m = 6$ (s) $d1, m = 6$ (t) $o1, m = 6$

Figure 6: Basins of attraction for test functions.

we use $p_5(z) = (z^2 + 3z + 5)^6$ with the zeros $z = \frac{1}{2}(-3 \pm i\sqrt{11})$. In Figure 6, the picture (d) has shown some black point and we find the considerable black point in (o), (s) and (t). The illustrative results are listed in Table 2 and Figure 6 .

We choose the equation $z = (\frac{x^8}{441} + \frac{8x^5}{63} - \frac{2857144357x^4}{50000000000} + \frac{16x^2}{9} - \frac{906122449x}{250000000} + \frac{3}{10})^4$ in Blood Rheology model[8] to carry out the experiments. The method y1 is better in view of con.

3. Discussion

Using an Möbius conjugacy map applied to a polynomial of the form $f(z) = (z-A)^m(z-B)^m$ with the multiplicity m, the complex dynamical analysis is investigated including the stability surfaces, the dynamical planes and the parameter spaces. We compare the proposed method with the existing iterative schemes. Based on the theoretical result, we experiment the test functions and draw the basins of attraction. The basins of attraction of this model are shown in Figure 5.

We will improve the current study to accurately address the visualization of diverse iterative schemes. In addition, the parameter space and basins of attraction of the developed multiple zero solver will be investigated in more detail. We will figure out the beautiful but complicated fractal generated by numerical iterative schemes from various perspectives.

Acknowledgements

The author is supported by Basic Science Research Program through the National Research Foundation of Korea funded by the Ministry of Education under the research grant(Project Number:NRF-2021R1A2C1012922)

Conflicts of Interest : The author declares no conflict of interest.

References

[1] L Ahlfors. *Complex Analysis.* McGraw-Hill Book Inc., 1979.

[2] S Amat, S Busquier, and S Plaza. *Iterative root-finding methods.* unpublished manuscript., 2004.

[3] I Argyros and A Magre nan. On the convergence of an optimal fourth-order family of methods and its dynamics. *Appl. Math. Comput.*, 252:336–346, 2015.

[4] A Beardon. *Iteration of Rational Functions.* Springer-Verlag, New York, 1991.

[5] R Behl, A Cordero, S Motsa, and J Torregrosa. On developing fourth-order optimal families of methods for multiple roots and their dynamics. *Appl. Math. Comput.*, 265:520–532, 2015.

[6] P Blanchard. The dynamics of newton's method. *Proceedings of Symposia in Appl. Math.*, 49:139–154, 1994.

[7] C.C.Dong. A basic theorem of constructing an iterative formula of the higher order for computing multiple roots of an euqation. *Mathematica Numerica Sinica*, 11:445–450, 1982.

[8] R.L. Fournier. *Basic transport phenomena in biomedical engineering.* CRC press., 2017.

[9] Y.H Geum and Y.I Kim. A cubic-order variant of newton's method for finding multiple roots of nonlinear equations. *Comput. Math. Appl.*, 62:1634–1640, 2011.

[10] V Kanwar, S Bhatia, and M Kansal. New optimal class of higher-order methods for multiple roots, permitting $f'(x_n) = 0$. *Appl. Math. Comput.*, 222(1):564–574, 2013.

[11] H.J. Kim, A.K. Rathie, and Y.H. Geum. A family of optimal cubic-order multiple-root solvers and their dynamics. *European Journal of Pure and Applied Mathematics*, 16(3):1902–1912, 2023.

[12] Y.I Kim and Y.H Geum. A triparametirc family of optimal fourth-order multiple-root finders and their dynamics. *J. Appl. Math.*, 8436759:1–23, 2016.

[13] Y.I Kim and Y.H Geum. Dynamical analysis via möbius conjugacy map on a uniparametric family of optimal fourth-order multiple-zero solvers with rational weight functions. *Discrete Dyn. Nature Soc.*, 7486125:1–19, 2018.

[14] S Kumar, V Kanwar, and S Singh. On some modified families of multipoint iterative methods for multiple roots of nonlinear equations. *Appl. Math. Comput.*, 218:7382–7394, 2012.

[15] S Li, X Liao, and L Cheng. A new fourth-order iterative method for finding multiple roots of nonlinear equations. *Appl. Math. Comput.*, 215:1288–1292, 2009.

[16] N Osada. An optimal multiple root-finding mehtod of order three. *J. Comput. Appl. Math.*, 51:131–133, 1994.

[17] A. M. Ostrowski. *Solutions of Equations and System of Equations.* Academic Press, New York, 1960.

[18] A. M. Ostrowski. *The Mathematica Book.* Wolfram Media, 5 edition, 2003.

[19] J. Traub. *Iterative Methods for the Solution of Equations.* Chelsea Publishing Company, 1997.

[20] J Wright, J Deane, M Bartucceli, and G Gentile. Basins of attraction in forced systems with time-varying dissipation. *Commun. Nonlinear Sci. Numer. Simul.*, 29(1-3):72–87, 2015.